Laser spectroscopy and cooling of Yb^+ ions on a deep-UV transition

Hendrik M. Meyer,* Matthias Steiner, Lothar Ratschbacher, Christoph Zipkes, and Michael Köhl
Cavendish Laboratory, University of Cambridge, JJ Thomson Avenue, Cambridge CB3 0HE, United Kingdom
(Received 1 December 2011; published 3 January 2012)

We perform laser spectroscopy of Yb^+ ions on the $4f^{14}6s\ ^2S_{1/2}$-$4f^{13}5d6s\ ^3D[3/2]_{1/2}$ transition at 297 nm. The frequency measurements for $^{170}Yb^+$, $^{172}Yb^+$, $^{174}Yb^+$, and $^{176}Yb^+$ reveal the specific mass shift as well as the field shifts. In addition, we demonstrate laser cooling of Yb^+ ions using this transition and show that light at 297 nm can be used as the second step in the photoionization of neutral Yb atoms.

DOI: 10.1103/PhysRevA.85.012502 PACS number(s): 32.30.−r

I. INTRODUCTION

In the last decade, trapped Yb^+ ions have been workhorses in the fields of quantum-information processing [1–3], precision measurements [4,5], and hybrid systems [6]. Yb^+ has a rich energy-level structure because besides pure valence-electron excitations, also electrons from a closed f shell can be excited. This leads to unusual features such as the electric octupole transition $^2S_{1/2}$-$^2F_{7/2}$, which is currently being explored for the prospect of an ion-based atomic clock, as it has a natural lifetime of several years [5,7].

Since the work of Ref. [8], a common feature of most trapped Yb^+ experiments is the continuous excitation of the ion within a four-level system (Fig. 1). The ion is cooled and detected on the $^2S_{1/2}$-$^2P_{1/2}$ transition near 369 nm. A second decay channel to the metastable $^2D_{3/2}$ state necessitates a second laser to avoid interruptions of the fluorescence. Light near 935 nm repopulates the ground state via the $^3D[3/2]_{1/2}$ state.

In this paper, we extend the available laser manipulation toolbox for trapped Yb^+ ions by exciting the $4f^{14}6s\ ^2S_{1/2}$-$4f^{13}5d6s\ ^3D[3/2]_{1/2}$ transition at 297 nm. We perform laser spectroscopy and present frequency measurements for four isotopes. The isotope shifts contain information about the change of the charge distribution within the nucleus and about the correlations of electrons, which are intricate because of a partially filled f shell in Yb^+. Therefore they can be used to test *ab initio* calculations. In addition, we show that the 297-nm light can be used as the second excitation step in the photoionization process of neutral Yb as well as for laser cooling of single Yb^+ ions. The relatively narrow linewidth could potentially allow one to reach lower laser cooling temperatures.

II. EXPERIMENTAL SETUP

We trap single Yb^+ ions in a rf Paul trap, which consists of two opposing end-cap electrodes [12] separated by 150 μm. The electrodes are formed from tungsten wire of 250 μm diameter and are etched to a needle-like geometry [13]. By applying a radio-frequency signal of 20 MHz and a few hundred volts amplitude, the ion is trapped with secular trap frequencies of $\omega_{ax}/2\pi \approx 3.7$ MHz and $\omega_{\mathrm{rad}}/2\pi \approx 1.7$ MHz. Single ions are loaded into the trap by two-step photoionization from a thermal atomic beam [14]. A stainless steel tube filled with Yb is resistively heated by a short current pulse (typically 60–80 ms, 60 A) and emits neutral Yb atoms into the trap. The atoms are resonantly excited on the $^1S_0$-$^1P_1$ transition with laser light at 398 nm and subsequently ionized by a laser at 369 nm. The first excitation step is isotope selective. After ionization, the ion is continuously laser cooled on the $^2S_{1/2}$-$^2P_{1/2}$ transition and the resulting fluorescence is collected by an in-vacuum objective and detected by a photomultiplier tube.

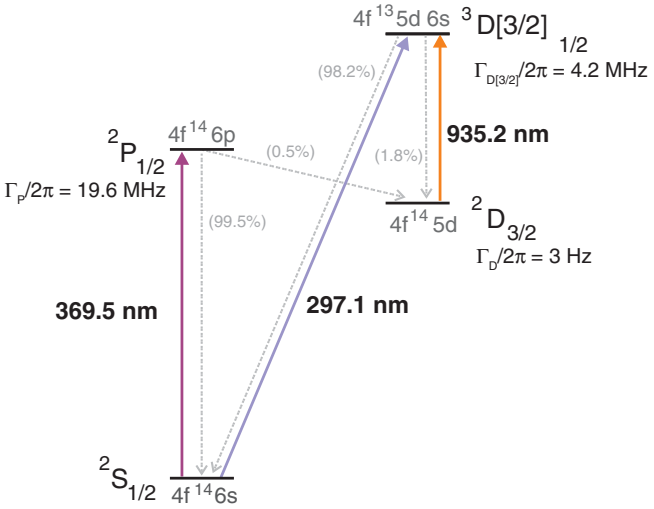

FIG. 1. (Color online) Relevant energy levels and transitions of Yb^+ (branching ratios given in percentages). $\Gamma_{D[3/2]}$, Γ_D, and branching ratio out of the $^2P_{1/2}$ state are taken from Ref. [9], $\Gamma_{D[3/2]}$ from Ref. [10], and the $^3D[3/2]_{1/2}$ branching ratio from Ref. [11].

The laser system for exciting the $^2S_{1/2}$-$^3D[3/2]_{1/2}$ transition at 297 nm is based on sum frequency generation (SFG) of light at 532 nm and 672 nm. The sketch of the optical setup is shown in Fig. 2. The green 532-nm laser is a commercial system (Coherent Verdi V6), whereas the red 672-nm diode laser with subsequent amplification stage is homebuilt. In order to supply an atomic frequency reference, the green laser is stabilized to the R(56)32-0 transition in molecular iodine [15]. As the study of isotope shifts in Yb^+ requires a large frequency scan range, we use the Doppler broadened absorption line (at room temperature: linewidth ≈ 0.8 GHz) and generate an error signal by FM spectroscopy [16]. We measured the rms frequency fluctuations of the green laser to be about 20 MHz.

*hmm39@cam.ac.uk

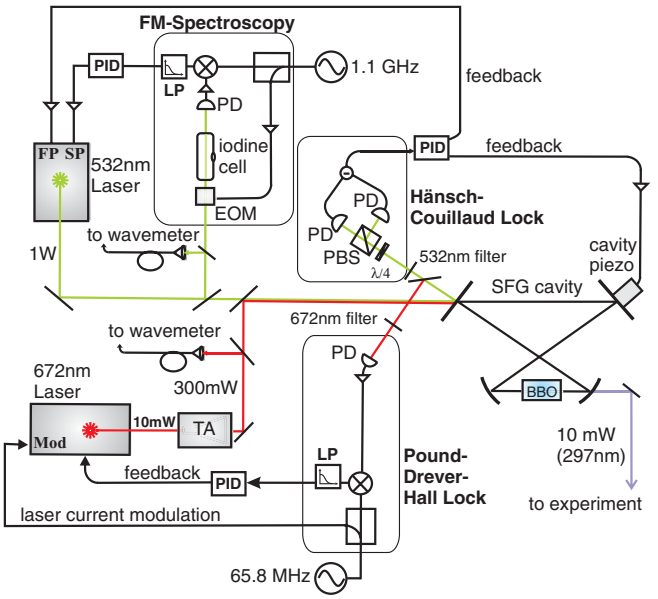

FIG. 2. (Color online) Laser system to generate 297-nm light. Abbreviations: BBO: Beta barium borate crystal, EOM: electro-optic modulator, FP: fast piezotransducer, LP: low pass, Mod: laser current modulation, PBS: polarizing beam splitter, PD: photodiode, PID: feedback controller, SFG: sum frequency generation, SP: slow piezotransducer, TA: tapered amplifier.

We achieve type-I (ooe) SFG in a doubly resonant bow-tie cavity (finesse: 75, free spectral range: 1.07 GHz). The cavity length is locked to the 532-nm laser using the Hänsch-Couillaud stabilization technique [17], whereas the 672-nm laser follows the SFG cavity by the Pound-Drever-Hall locking technique [18]. By sweeping the green 532-nm laser we can scan the generated UV light continuously about 1 GHz. Input light intensities of 1 W (532 nm) and 300 mW (672 nm) yield about 10 mW of 297-nm light.

III. ISOTOPE SHIFTS

Spectroscopy on the $^2S_{1/2}$-$^3D[3/2]_{1/2}$ transition is performed in a double-resonance scheme. The laser at 369 nm cools the ion continuously on the $^2S_{1/2}$-$^2P_{1/2}$ transition and yields fluorescence, which is detected. Simultaneously, the 297-nm probe laser excites the $^2S_{1/2}$-$^3D[3/2]_{1/2}$ transition. Additional 935-nm light is necessary to deplete the population of the $^3D[3/2]_{1/2}$ state. By sweeping the frequency of the 297-nm light, the $^2S_{1/2}$-$^3D[3/2]_{1/2}$ resonance is observed as a decrease in the 369-nm fluorescence (Fig. 3).

The ratio of the saturation parameters, $s_{369\,\mathrm{nm}}$ and $s_{297\,\mathrm{nm}}$ [$s_\lambda = \frac{I_\lambda}{I_{\lambda,\,\mathrm{sat}}}$, with the (saturation) intensity I_λ ($I_{\lambda,\,\mathrm{sat}}$)] is important for the strength of the observed signal. For similar saturation parameters $s_{369\,\mathrm{nm}} \approx s_{297\,\mathrm{nm}}$, the $^2S_{1/2}$-$^2P_{1/2}$ fluorescence shows a significant drop. The steady-state fluorescence is proportional to the population of the $^2P_{1/2}$ state, which is given by

$$p_P = \frac{1}{2}\frac{s_{369\,\mathrm{nm}}}{1 + s_{369\,\mathrm{nm}} + \left(\frac{2\Delta_{369\,\mathrm{nm}}}{\Gamma_P}\right)^2 + \epsilon}, \qquad (1)$$

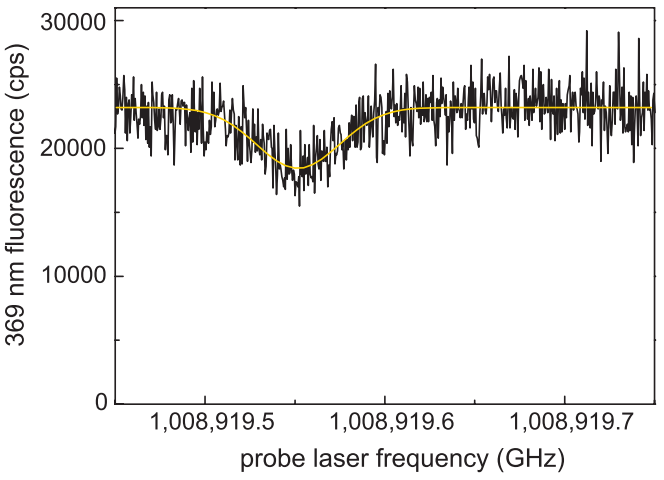

FIG. 3. (Color online) Double-resonance spectrum of the $^2S_{1/2}$-$^3D[3/2]_{1/2}$ transition in $^{176}Yb^+$. Yellow (grey) line: Gauss fit. Transition frequencies have been determined by averaging ten spectra.

assuming fast repumping out of the $^2D_{3/2}$ state and neglecting coherences. Here $\Delta_{369\,\mathrm{nm}}$ is the detuning of the 369-nm laser and Γ_P the natural linewidth of the $^2P_{1/2}$ state. The term ϵ describes the coupling to the $^3D[3/2]_{1/2}$ state

$$\epsilon = \frac{1}{2}\frac{s_{297\,\mathrm{nm}}\left[2 + s_{369\,\mathrm{nm}} + 2\left(\frac{2\Delta_{369\,\mathrm{nm}}}{\Gamma_P}\right)^2\right]}{2 + s_{297\,\mathrm{nm}} + 2\left(\frac{2\Delta_{297\,\mathrm{nm}}}{\Gamma_{D[3/2]}}\right)^2}, \qquad (2)$$

where $\Delta_{297\,\mathrm{nm}}$ is the detuning of the 297-nm laser and $\Gamma_{D[3/2]}$ the natural linewidth of the $^3D[3/2]_{1/2}$ state. For typical experimental parameters of $s_{369\,\mathrm{nm}} \approx s_{297\,\mathrm{nm}} \approx 1$–4 and $\Delta_{369\,\mathrm{nm}} \approx -\Gamma_P/2$, this results in a 10–30% drop of the fluorescence, which is consistent with our measured spectra. We typically scan the 297-nm light 400 MHz in 10 s and record the 369-nm fluorescence. The linewidth of the 297-nm laser, residual micromotion, and the continuous driving of the $^2S_{1/2}$-$^2P_{1/2}$ transition broaden the linewidth, which is measured to be 40 MHz. The absolute frequency is determined by measuring the frequency of the 532-nm and 672-nm lasers with a wave meter (HighFinesse WS/07). The wave meter is calibrated to the D_2 [$F = 2$, $F' = (2,3)$] crossover line in ^{87}Rb and has a specified 3-σ accuracy of 60 MHz. In this manner we measured the $^2S_{1/2}$-$^3D[3/2]_{1/2}$ frequencies for the isotopes $^{170}Yb^+$, $^{172}Yb^+$, $^{174}Yb^+$, and $^{176}Yb^+$ (Table I). The uncertainty of the measured frequencies is mainly determined by the accuracy of the wave meter. The light shift caused by the lights at 369 and 935 nm is calculated to be below 10 MHz for the laser intensities used.

TABLE I. Measured frequencies of the $^2S_{1/2}$-$^3D[3/2]_{1/2}$ transition in Yb^+ (1-σ error).

Isotope	Frequency (THz)
$^{170}Yb^+$	1008.916 19(3)
$^{172}Yb^+$	1008.917 59(3)
$^{174}Yb^+$	1008.918 55(3)
$^{176}Yb^+$	1008.919 58(3)

The isotope shift of a spectral line consists of two contributions: the field and the mass shift [19]. The field shift (FS) is caused by the change of the charge distribution within the nucleus and is very sensitive to the electron charge density at the nucleus $|\Psi(0)|^2$. The mass shift itself has two contributions: the change in the reduced mass is taken into account by the normal mass shift (NMS), whereas the specific mass shift (SMS) describes the change in the correlations between electrons. In total, the isotope shift of a spectral line α between isotopes a and b reads

$$\Delta\nu^{\alpha}_{a,b} = \delta\nu^{\alpha}_{\mathrm{FS},a,b} + \left(k^{\alpha}_{\mathrm{NMS}} + k^{\alpha}_{\mathrm{SMS}}\right)\frac{M_b - M_a}{M_a(M_b + m_e)}, \quad (3)$$

with M_a and M_b ($M_a < M_b$) being the isotope masses and m_e the mass of the electron. The parameter $k^{\alpha}_{\mathrm{NMS}}$ depends only on the transition frequency of the lighter isotope ν_a and is given by $k^{\alpha}_{\mathrm{NMS}} = \nu^{\alpha}_a m_e$. A common technique used to identify the field shift and the specific mass shift from measured isotope shifts $\Delta\nu^{\alpha}_{a,b}$ is via a King plot [19]. After eliminating the normal mass shift from the measured isotope shift, the residual shift is multiplied by $\frac{M_a(M_b+m_e)}{M_b-M_a}$ and the reduced mass of a reference pair (we choose ^{170}Yb and ^{174}Yb) to obtain the modified isotope shift $\Delta\widetilde{\nu}^{\alpha}_{a,b}$:

$$\Delta\widetilde{\nu}^{\alpha}_{a,b} = \frac{M_{174} - M_{170}}{M_{170}(M_{174} + m_e)} \times \left(\frac{M_a(M_b + m_e)}{M_b - M_a}\Delta\nu^{\alpha}_{a,b} - \nu^{\alpha}_a m_e\right). \quad (4)$$

The modified isotope shift $\widetilde{\nu}^{\alpha}_{a,b}$ is plotted against that of another transition β and the slope γ of the resulting linear fit relates the field shifts:

$$\gamma = \frac{\delta\nu^{\alpha}_{\mathrm{FS},a,b}}{\delta\nu^{\beta}_{\mathrm{FS},a,b}}. \quad (5)$$

We use the data from Clark *et al.* [20] on the 555.6-nm $^1S_0$-$^3P_1$ transition in neutral Yb as the reference for the King plot. These data are very precise and allow us to calculate the field shift [21]. For the King plot and the determination of the transition characteristic parameter, $\delta\nu^{\alpha}_{\mathrm{FS},a,b}$ and $k^{\alpha}_{\mathrm{SMS}}$, ^{170}Yb was chosen as the reference isotope. From Fig. 4 we extract the slope $\gamma = -1.26(20)$ and calculate $\delta\nu^{297\mathrm{nm}}_{\mathrm{FS},a,b}$ and $k^{297\mathrm{nm}}_{\mathrm{SMS}}$ (Table II).

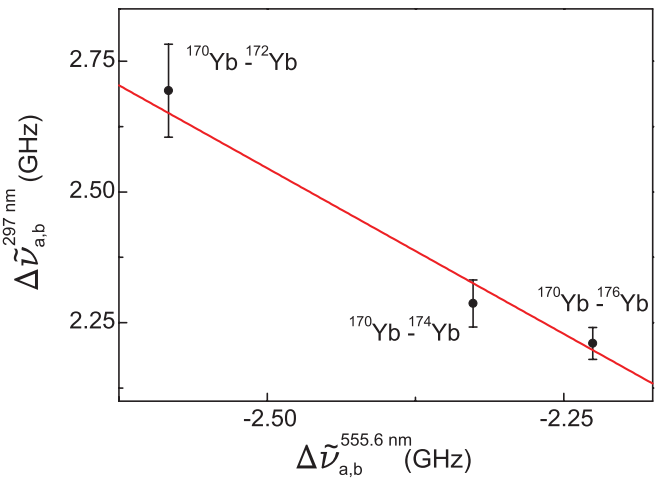

FIG. 4. (Color online) King plot of our data vs the data of Clark *et al.* [20]. The slope of the linear fit is used to determine the field shift.

TABLE II. Experimentally determined contributions to the isotope shift.

$\delta\nu^{297\ \mathrm{nm}}_{\mathrm{FS},170,176}$	4.16(66) GHz
$\delta\nu^{297\ \mathrm{nm}}_{\mathrm{FS},170,174}$	2.92(47) GHz
$\delta\nu^{297\ \mathrm{nm}}_{\mathrm{FS},170,172}$	1.65(26) GHz
$k^{297\ \mathrm{nm}}_{\mathrm{SMS}}$	−4.5(4.0) GHz amu

Our results can be interpreted in comparison with the data of Zinkstok *et al.* [21], who investigated a similar line in neutral Yb, namely, the $4f^{14}6s^2\ ^1S_0$ to $4f^{13}5d6s^2\ ^1P_1$ transition. They found a similarly large negative specific mass shift, which is explained by the strong coupling of d and f electrons [19]. In contrast, our measured field shift is about 50% higher. This may reflect the fact that, in general, the electron charge density at the nucleus is higher in ionic systems than in their neutral counterparts and thereby more sensitive to changes of the charge distribution within the nucleus.

IV. PHOTOIONIZATION AND LASER COOLING

Photoionization of Yb can be achieved by a photon at 398 nm ($^1S_0$-$^1P_1$ transition) and a second photon with a wavelength smaller than 394 nm. Here we demonstrate that light at 297 nm can be used for the second step. At the beginning of the loading sequence the Yb oven is heated for 75 ms and simultaneously the 398, 297, and 935-nm laser lights are switched on. After 3 s the light at 398 nm is turned off, and 1 s later the 369-nm laser illuminates the ion and the resulting fluorescence is recorded (Fig. 5). We note that for

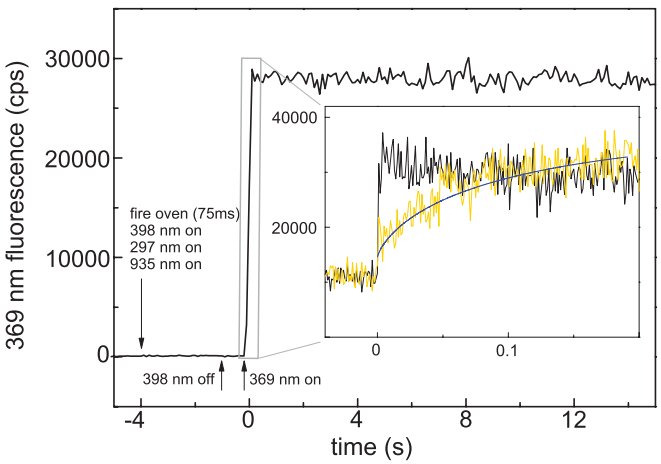

FIG. 5. (Color online) Recorded 369-nm fluorescence while loading a single Yb$^+$ with 297-nm light. Inset: Zoom into the onset of the fluorescence (each curve is the average of ten loadings). Yellow (light grey) curve: large detuning, $\Delta_{297\ \mathrm{nm}} = -400$ MHz. Blue (dark grey) line: expected fluorescence of a 100 K hot ion [22]. Black curve: sweep of $\Delta_{297\ \mathrm{nm}}$ from −200 to −60 MHz in 3 s after heating the oven leads to a high initial level of 369-nm fluorescence indicating a cold ion. In both cases $\Delta_{369\ \mathrm{nm}} = -\Gamma_P/2$.

reliable loading, the oven heating time needs to be slightly longer than that for standard loading with 369-nm light.

The fluorescence curve after switching on the 369-nm light depends strongly on the kinetic energy of the ion due to the Doppler shift and can be used to determine its temperature [22,23]. To measure the onset of fluorescence, we interrupt the 935-nm light 10 ms before the 369-nm light is switched on. This allows the 369-nm intensity controller to adjust without affecting the ion. We switch the 935-nm light back on 100 ms later. Only with both lights, 935 and 369 nm, the excitation cycle is closed and the ion continuously scatters photons. The inset in Fig. 5 shows the onset of the fluorescence for two different loading sequences. In the first the 297-nm laser is set 400 MHz below the resonance frequency during the loading. Because of the large detuning the ion scatters only a few photons on the $^2S_{1/2}$-$^3D[3/2]_{1/2}$ transition and the cooling of the ion is very inefficient. Thus, the 369 nm fluorescence starts low due to Doppler broadening and increases as the 369-nm laser cools the ion. In the second loading sequence, a smooth shifting of the 297-nm laser frequency toward the resonance (from $\Delta_{297\,\mathrm{nm}} = -200$ MHz to $\Delta_{297\,\mathrm{nm}} = -60$ MHz) in the first 3 s after photoionization yields a photon scatter rate, which starts immediately at its saturation value and hence indicates a cold ion.

V. CONCLUSION

In conclusion, we have demonstrated laser spectroscopy, photoionization, and laser cooling of a single Yb^+ ion on the $4f^{14}6s\ ^2S_{1/2}$-$4f^{13}5d6s\ ^3D[3/2]_{1/2}$ transition. We measure the isotope shifts and determine the specific mass shift as well as the field shifts. The results on loading and cooling show that this transition complements the existing manipulation capabilities of Yb^+ ions and potentially could replace the $^2S_{1/2}$-$^2P_{1/2}$ transition. In the future, we plan to make use of the relatively narrow line width of this transition to facilitate Doppler cooling to very low temperatures, potentially directly into the vibrational ground state. Moreover, the new availability of a Λ system in Yb^+ will allow new ways of quantum state manipulation and, for example, EIT cooling [24,25].

ACKNOWLEDGMENTS

We thank Sebastien Garcia, Neil McDonald, Ben Metcalf, Christopher Overstreet, and the workshop of the Cavendish Laboratory. This work has been supported by EPSRC (EP/H005679/1) and ERC (Grant No. 240335).

[1] D. L. Moehring, P. Maunz, S. Olmschenk, K. C. Younge, D. N. Matsukevich, L.-M. Duan, and C. Monroe, Nature **449**, 68 (2007).
[2] K. Kim, M.-S. Chang, S. Korenblit, R. Islam, E. E. Edwards, J. K. Freericks, G.-D. Lin, L.-M. Duan, and C. Monroe, Nature **465**, 590 (2010).
[3] N. Timoney, I. Baumgart, M. Johanning, A. F. Varon, M. B. Plenio, A. Retzker, and C. Wunderlich, Nature **476**, 185 (2011).
[4] T. Schneider, E. Peik, and C. Tamm, Phys. Rev. Lett. **94**, 230801 (2005).
[5] M. Roberts, P. Taylor, G. P. Barwood, W. R. C. Rowley, and P. Gill, Phys. Rev. A **62**, 020501 (2000).
[6] C. Zipkes, S. Palzer, C. Sias, and M. Köhl, Nature **464**, 388 (2010).
[7] M. Roberts, P. Taylor, G. P. Barwood, P. Gill, H. A. Klein, and W. R. C. Rowley, Phys. Rev. Lett. **78**, 1876 (1997).
[8] A. S. Bell, P. Gill, H. A. Klein, A. P. Levick, C. Tamm, and D. Schnier, Phys. Rev. A **44**, R20 (1991).
[9] S. Olmschenk, K. C. Younge, D. L. Moehring, D. N. Matsukevich, P. Maunz, and C. Monroe, Phys. Rev. A **76**, 052314 (2007).
[10] R. W. Berends, E. H. Pinnington, B. Guo, and Q. Ji, J. Phys. B **26**, L701 (1993).
[11] E. Biémont, J.-F. Dutrieux, I. Martin, and P. Quinet, J. Phys. B **31**, 3321 (1998).
[12] C. Schrama, E. Peik, W. Smith, and H. Walther, Opt. Commun. **101**, 32 (1993).
[13] L. Deslauriers, S. Olmschenk, D. Stick, W. K. Hensinger, J. Sterk, and C. Monroe, Phys. Rev. Lett. **97**, 103007 (2006).
[14] C. Balzer, A. Braun, T. Hannemann, C. Paape, M. Ettler, W. Neuhauser, and C. Wunderlich, Phys. Rev. A **73**, 041407 (2006).
[15] P. Jungner, S. Swartz, M. Eickhoff, J. Ye, J. Hall, and S. Waltman, IEEE Trans. Instrum. Meas. **44**, 151 (1995).
[16] G. C. Bjorklund, M. D. Levenson, W. Lenth, and C. Ortiz, Appl. Phys. B **32**, 145 (1983).
[17] T. Hänsch and B. Couillaud, Opt. Commun. **35**, 441 (1980).
[18] R. W. P. Drever, J. L. Hall, F. V. Kowalski, J. Hough, G. M. Ford, A. J. Munley, and H. Ward, Appl. Phys. B **31**, 97 (1983).
[19] W. H. King, *Isotope Shifts in Atomic Spectra* (Plenum, New York, 1984).
[20] D. L. Clark, M. E. Cage, D. A. Lewis, and G. W. Greenlees, Phys. Rev. A **20**, 239 (1979).
[21] R. Zinkstok, E. J. van Duijn, S. Witte, and W. Hogervorst, J. Phys. B **35**, 2693 (2002).
[22] J. H. Wesenberg *et al.*, Phys. Rev. A **76**, 053416 (2007).
[23] R. J. Epstein *et al.*, Phys. Rev. A **76**, 033411 (2007).
[24] G. Morigi, J. Eschner, and C. H. Keitel, Phys. Rev. Lett. **85**, 4458 (2000).
[25] C. F. Roos, D. Leibfried, A. Mundt, F. Schmidt-Kaler, J. Eschner, and R. Blatt, Phys. Rev. Lett. **85**, 5547 (2000).